

Statistical ensembles and molecular dynamics studies of anisotropic solids. II

John R. Ray, and Aneesur Rahman

Citation: [The Journal of Chemical Physics](#) **82**, 4243 (1985); doi: 10.1063/1.448813

View online: <https://doi.org/10.1063/1.448813>

View Table of Contents: <http://aip.scitation.org/toc/jcp/82/9>

Published by the [American Institute of Physics](#)

Articles you may be interested in

[Statistical ensembles and molecular dynamics studies of anisotropic solids](#)

The Journal of Chemical Physics **80**, 4423 (1984); 10.1063/1.447221

[Strain fluctuations and elastic constants](#)

The Journal of Chemical Physics **76**, 2662 (1982); 10.1063/1.443248

[Generalized expressions for the calculation of elastic constants by computer simulation](#)

Journal of Applied Physics **65**, 2991 (1989); 10.1063/1.342716

[Molecular dynamics simulations at constant pressure and/or temperature](#)

The Journal of Chemical Physics **72**, 2384 (1980); 10.1063/1.439486

[Fluctuations and thermodynamic properties of anisotropic solids](#)

Journal of Applied Physics **53**, 6441 (1982); 10.1063/1.331517

[Molecular dynamics with coupling to an external bath](#)

The Journal of Chemical Physics **81**, 3684 (1984); 10.1063/1.448118

PHYSICS TODAY

WHITEPAPERS

ADVANCED LIGHT CURE ADHESIVES

Take a closer look at what these
environmentally friendly adhesive
systems can do

READ NOW

PRESENTED BY



Statistical ensembles and molecular dynamics studies of anisotropic solids. II^{a)}

John R. Ray^{b)} and Aneesur Rahman

Argonne National Laboratory, Argonne, Illinois 60439

(Received 5 November 1984; accepted 14 January 1985)

We have recently discussed how the Parrinello–Rahman theory can be brought into accord with the theory of the elastic and thermodynamic behavior of anisotropic media. This involves the isoenthalpic–isotension ensemble of statistical mechanics. Nosé has developed a canonical ensemble form of molecular dynamics. We combine Nosé's ideas with the Parrinello–Rahman theory to obtain a canonical form of molecular dynamics appropriate to the study of anisotropic media subjected to arbitrary external stress. We employ this isothermal–isotension ensemble in a study of a fcc→close-packed structural phase transformation in a Lennard-Jones solid subjected to uniaxial compression. Our interpretation of the Nosé theory does not involve a scaling of the time variable. This latter fact leads to simplifications when studying the time dependence of quantities.

I. INTRODUCTION

In a recent paper¹ we have shown how the molecular dynamics theory developed by Parrinello and Rahman² can be put into accord with the theory of finite elasticity. The ensemble generated by this molecular dynamics theory is the isoenthalpic–isotension or (*HtN*) ensemble. Here *H* is the enthalpy of the theory of elasticity of anisotropic media,³ *t* the thermodynamic tension, and *N* the particle number.

Recently Nosé⁴ has presented a new form of molecular dynamics which generates the canonical ensemble. The modifications needed in the (*HtN*) molecular dynamics to convert it into a canonical (*TtN*) ensemble where *T* is the assigned temperature are presented here. As an example of this theory we employ it to study a solid→solid structural phase transformation in a low temperature Lennard-Jones solid. For convenience we shall adopt the notation and terminology entirely as in Ref. 1. [Note that in Ref. 1 Eq. (2.6) should have a minus sign before the first term on the right-hand side, that is, the correct equation is Eq. (2.2) below.]

II. THE (*HtN*) THEORY

The Hamiltonian which generates the (*HtN*) ensemble may be written

$$\mathcal{H}_1(\mathbf{s}, \boldsymbol{\pi}, h, \Pi) = \frac{1}{2} \sum_a \pi'_a G^{-1} \pi_a / m_a + \sum_{a < b} U(r_{ab}) + \frac{1}{2} \text{Tr } \Pi' \Pi / W + V_0 \text{Tr } t \epsilon. \quad (2.1)$$

The equations of motion which follow from this Hamiltonian have the form

$$m_a \ddot{s}_a = - \sum \chi_{ab} s_{ab} - m_a G^{-1} \dot{G} \dot{s}_a, \quad (2.2)$$

$$W \ddot{h} = \mathcal{P} A - h \Gamma. \quad (2.3)$$

In the new approach by Nosé⁴ one introduces another degree of freedom *f*(*t*). We shall associate this new degree of

freedom with the particle masses *m_a* as will be seen below. This new degree of freedom is given a kinetic energy $\frac{1}{2} P^2 / M$, where *M* is a constant and *P* = *Mf* is the canonical momentum conjugate of *f*. The new degree of freedom is also given a potential energy $(F + 1) k_B T_0 \ln f$, where *T₀* is the preassigned temperature and *F* is the number of degrees of freedom of the particles in the physical system (*F* = 3*N* for *N* particles in three dimensions). Note that the degrees of freedom associated with *h* do not enter into *F*.

III. THE (*TtN*) THEORY

The Hamiltonian for the (*TtN*) ensemble is postulated to be

$$\mathcal{H}_2(\mathbf{s}, \boldsymbol{\pi}, h, \Pi, f, P) = \frac{1}{2} \sum_a \pi'_a G^{-1} \pi_a / (m_a f^2) + \sum_{a < b} U(r_{ab}) + \frac{\text{Tr } \Pi' \Pi}{2W} + V_0 \text{Tr } t \epsilon + \frac{1}{2} P^2 / M + (F + 1) k_B T_0 \ln f. \quad (3.1)$$

For the sake of simplicity of notation the preassigned temperature occurring in Eq. (3.1) is written simply as *T* when denoting the ensemble (*TtN*). Note the manner in which the new dynamical variable of Nosé has been introduced into Eq. (3.1). This Hamiltonian can be obtained using the methods of Ref. 1 by: (1) carrying out a canonical transformation on the particle Hamiltonian as in Ref. 1, and a mass scaling: *m_a*→*m_a* *f*², (2) adding to this Hamiltonian, kinetic and potential energy terms for the new degrees of freedom which are introduced, which are *h* and *f*.

The new equations of motion which follow from Eq. (3.1) have the form

$$m_a f^2 \ddot{s}_a = - \sum \chi_{ab} s_{ab} - m_a (f^2 G^{-1} \dot{G} + 2f \dot{f}) \dot{s}_a, \quad (3.2)$$

$$W \ddot{h} = \mathcal{P} A - h \Gamma, \quad (3.3)$$

$$M \ddot{f} = 2K / f - (F + 1) k_B T_0 / f, \quad (3.4)$$

where *K* is the particle kinetic energy

$$K = \frac{1}{2} \sum \dot{\pi}_a^2 / m_a, \quad (3.5)$$

^{a)} Work supported by the U.S. Department of Energy.

^{b)} Permanent address: Department of Physics and Astronomy, Clemson University, Clemson, South Carolina 29631.

and the momentum ρ_a being defined by $\rho_a = m_a f \dot{h}_a$. This momentum appears in the kinetic energy Eq. (3.5) and also in the microscopic stress tensor \mathcal{P}_{ij} occurring in Eq. (3.3):

$$\mathcal{P}_{ij} = V^{-1} \left(\sum_a \rho_{ai} \rho_{aj} / m_a - \sum \chi_{ab} r_{abi} r_{abj} \right). \quad (3.6)$$

Therefore, we shall refer to ρ_a as the *physical momentum* of the particle in order to distinguish it from various other momenta that occur in the theory.

The "masses" W and M are introduced in order to obtain dynamical equations for the variables h and f .

The importance of the Nosé choice of the logarithmic potential for the variable f appears if we calculate the average value of a function of the physical momentum ρ_a , of the position $x_a = h s_a$, and of h using the dynamical equations (3.2)–(3.4). Since these equations define a microcanonical ensemble with energy \mathcal{H}_2 we have

$$\overline{A(x, \rho, h)} = \frac{\int A(x, \rho, h) \delta(\mathcal{H}_2 - E) df dP dh_{ij} d\Pi_{ij} d^F s_a d^F \pi_a}{\int \delta(\mathcal{H}_2 - E) df dP dh_{ij} d\Pi_{ij} d^F s_a d^F \pi_a}. \quad (3.7)$$

For the integrals on the right we carry out the inverse of the canonical transformation, mentioned before Eq. (3.2), along with a change of variables using $f: \rho_a = h^{-1} \pi_a / f$, $x_a = h s_a$. The relationship $\rho_a = h^{-1} \pi_a / f$ is just the connection between the physical momentum ρ_a mentioned above and the canonical momentum π_a . Carrying out this change of variables, performing the same steps as in Nosé, Ref. 4, and writing $\mathcal{H} = \frac{1}{2} \sum \rho_a^2 / m_a + \sum U + V_0 \text{Tr} \epsilon$ we find

$$\overline{A} = \frac{\int A(x, \rho, h) e^{-\mathcal{H}/k_B T_0} d^F x_a d^F \rho_a dh_{ij}}{\int e^{-\mathcal{H}/k_B T_0} d^F x_a d^F \rho_a dh_{ij}}. \quad (3.8)$$

The right-hand side of Eq. (3.8) is just the (TtN) ensemble average of $A(x, \rho, h)$,

$$\overline{A} = \langle A \rangle_{(TtN)}. \quad (3.9)$$

Thus, the average calculated using the trajectories generated by the dynamical equations (3.2), (3.3), and (3.4) is equal to the canonical ensemble (TtN) average of A .

One can also formulate a (TPN) ensemble as mentioned by Nosé. As has already been explained in some detail (Ref. 1) the (TPN) ensemble is not a special case of the (TtN) ensemble because of the manner in which enthalpy is defined in the elasticity theory for anisotropic media.³ In other words the (TPN) and (TtN) ensembles have to be dealt with as appropriate and not to expect that one is a special case of the other. The same statement is also true for the (HPN) and (HtN) ensembles.

Note, however, that if one applies an isotropic pressure P to a system which has a tension t applied to it then the proper enthalpy involves the sum $PV + V_0 \text{Tr}(\epsilon t)$. This sum would replace the term $V_0 \text{Tr}(\epsilon t)$ in Eqs. (2.1) and (3.1). The equation of motion for h in this combined case has the form

$$W \ddot{h} = (\mathcal{P} - P)A - \Gamma h \quad (3.10)$$

for both Hamiltonians (2.1) and (3.1). The other equations of motion for these Hamiltonians in this case of combined ex-

ternal influences are the same as given earlier; namely Eq. (2.2) for Hamiltonian, equation (2.1), and Eqs. (3.2) and (3.4) for Hamiltonian, equation (3.1). Thus, in this case where one has a combination of external hydrostatic pressure and tension the molecular dynamics equations generate an (Ht) and (PN) for Eq. (2.1) or (Tt) and (PN) for Eq. (3.1) ensemble. The definition of the enthalpy in the manner just described insures that our results are consistent with thermodynamic conventions chosen in the theory of anisotropic media. For simplicity of discussion in the rest of this paper we shall not mention these "combination" ensembles further but leave it understood that one may always make use of them.

IV. THE (EhN) AND (ThN) THEORY

The tensor h can be constrained to remain constant, i.e., not vary with time; then the Hamiltonian equation (2.1) generates the (EhN) ensemble of conventional molecular dynamics which has been discussed in Ref. 1. If $h = \text{constant}$ in \mathcal{H}_2 then just the two dynamical equations (3.2) and (3.4) need to be solved, with the G term being absent in Eq. (3.2). The average values using these trajectories are equal to averages in the (ThN) canonical ensemble:

$$\begin{aligned} \overline{A(x, \rho)} &= \frac{\int A(x, \rho) \delta(\mathcal{H}_2 - E) df dP d^F s_a d^F \pi_a}{\int \delta(\mathcal{H}_2 - E) df dP d^F s_a d^F \pi_a} \\ &= \frac{\int A(x, \rho) e^{-\mathcal{H}/k_B T_0} d^F x_a d^F \rho_a}{\int e^{-\mathcal{H}/k_B T_0} d^F x_a d^F \rho_a}, \end{aligned} \quad (4.1)$$

where again the transformation $x_a = h s_a$, $\rho_a = h^{-1} \pi_a / f$ has been employed and $\mathcal{H} = \frac{1}{2} \sum \rho_a^2 / m_a + \sum U(r_{ab})$ (note that here h is a constant). Equation (4.1) implies that the averages calculated using the trajectories arising from dynamical equations (3.2) and (3.4) only are equal to averages in the canonical (ThN) ensemble

$$\overline{A} = \langle A \rangle_{(ThN)}. \quad (4.2)$$

Using Eq. (3.9) [or its (TPN) counterpart] one now has a direct way of comparing molecular dynamics averages and Monte Carlo averages for the (TtN) ensemble. Similarly using Eq. (4.2) one can compare molecular dynamics and Monte Carlo averages in the (ThN) , that is, the usual canonical ensemble.

There are, of course, many fluctuation formulas in the (TtN) and (ThN) ensembles. As an example the *isothermal* compliances C_{ijkl}^{-1} can be determined in the (TtN) ensemble by the fluctuation in strain

$$\overline{\epsilon_{ij} \epsilon_{kl}} - \bar{\epsilon}_{ij} \bar{\epsilon}_{kl} = k_B T C_{ijkl}^{-1} / V_0. \quad (4.3)$$

The (HtN) form of this fluctuation formula was first given by Parrinello and Rahman.⁵

V. STUDY OF A STRUCTURAL PHASE TRANSFORMATION IN THE (TtN) ENSEMBLE

A. General discussion

We have performed several molecular dynamics calculations using Eqs. (3.2), (3.3), and (3.4) of the (TtN) ensemble. A 500 particle system interacting with the Lennard-Jones (12-6) potential was employed; henceforth we shall use the conventional reduced units.

The calculation we discuss exhibits a structural phase

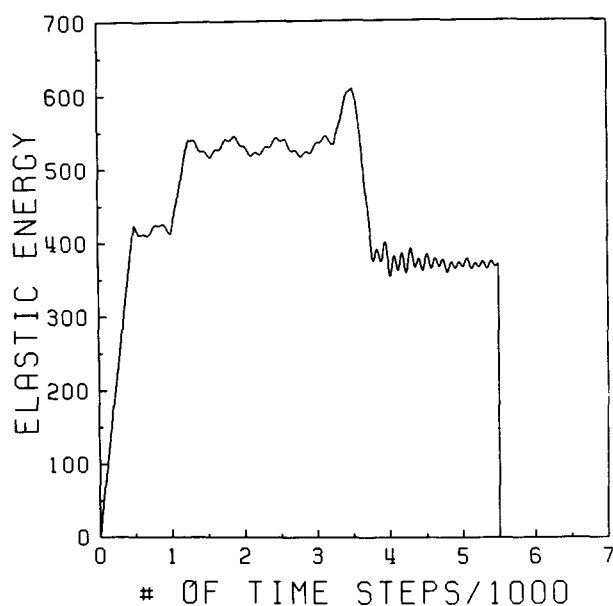


FIG. 1. The time history of the elastic energy stored in the system.

transformation from fcc to a close-packed structure with stacking faults under compressive uniaxial loading along the [100] direction. Parrinello and Rahman² first studied such transformations using the (HtN) ensemble, i.e., Eqs. (3.2) and (3.3), only. Their study was for a Morse potential model of a single crystal of "nickel" and they used a 500 particle system.

We prepared an fcc lattice of particles in an unstressed state at a temperature of approximately $T_0 = 0.15$. Uniaxial compression along the [100] direction was then applied resulting in the structural phase transformation fcc \rightarrow close-packed structure at a value of Γ between 20 and 25. We recall that Γ is the constant, externally applied stress tensor appearing in Eq. (3.3). In the calculations reported in this paper the only nonzero component of the tensor is Γ_{11} . For simplicity of notation we shall denote Γ_{11} by Γ in this paper. In Figs. 1–4 we show the variation of the elastic energy,

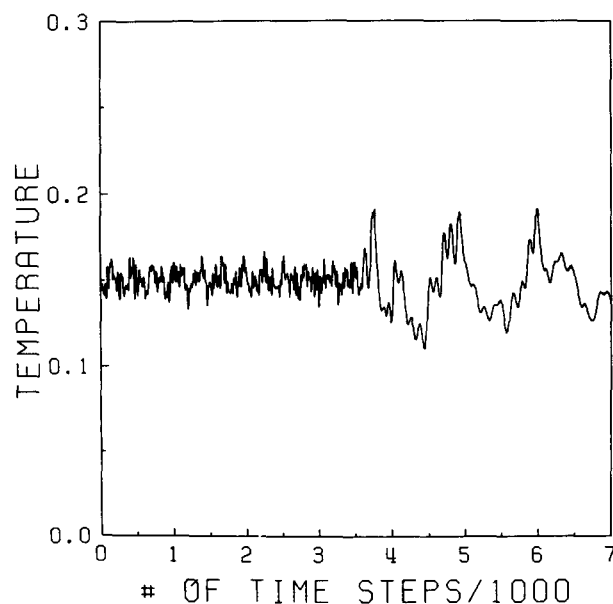
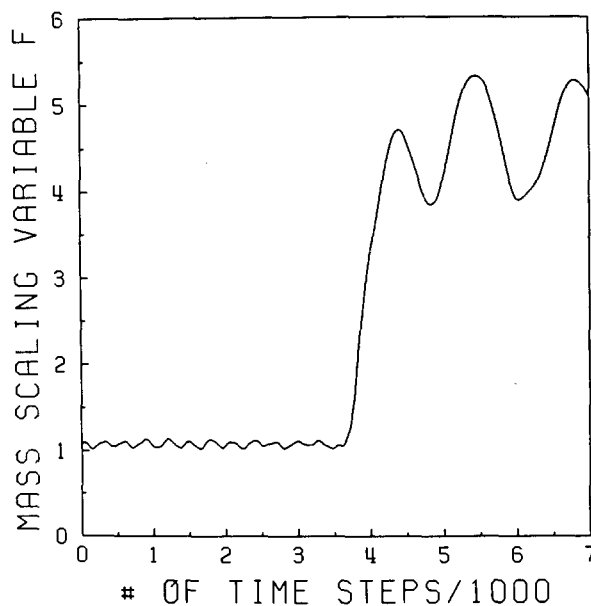


FIG. 2. The time history of the instantaneous temperature.

FIG. 3. The time history of the Nosé variable f .

temperature, Nosé's scaling variable f , and the mean square displacement as functions of time before and after the transformation.

Note the manner in which we have used the new dynamical variable f ; it is used as a mass scaling device and *not* for scaling time. This obviously has the advantage of simplicity in studying the time dependence of the various quantities of interest. We shall return to the question of the interpretation of f in the conclusions.

The system was allowed to equilibrate for 1500 time steps under zero stress, each time step being $\Delta t = 0.005$. As is usual in all such studies the figures do not display the period of time of equilibration, after which the data is recorded for later detailed study.

The following is a detailed discussion of the manner in which the compressive uniaxial load was applied to the system. The stress was applied by increasing Γ by 0.03 units

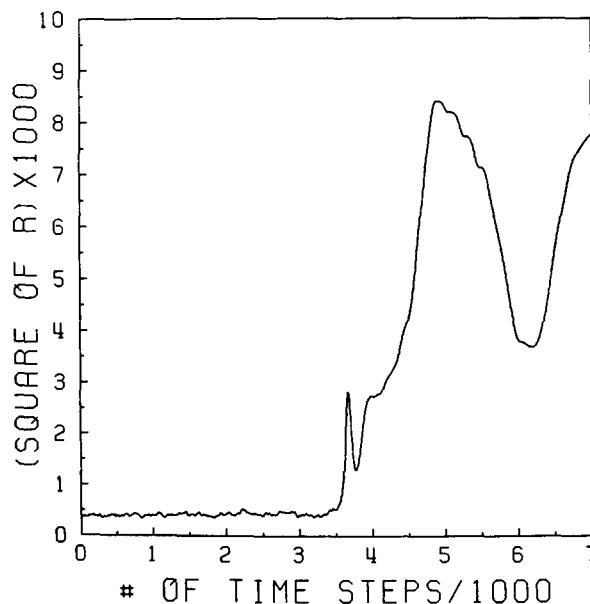


FIG. 4. The time history of the mean square displacement.

every time step for $500 \Delta t$, thus building the stress Γ up to a value of 15. Then the system was allowed to evolve via Eqs. (3.2), (3.3), and (3.4) with $\Gamma = 15$ for $500 \Delta t$. Next the stress was increased by 0.02 units for $250 \Delta t$ so that the value $\Gamma = 20$ was obtained. The system then evolved for $2000 \Delta t$ with $\Gamma = 20$. Next the stress was increased by 0.02 units per time step for $250 \Delta t$, thus achieving a final value of $\Gamma = 25$ at time step 3500. From $3500 \Delta t$ up to $5500 \Delta t$ the system was allowed to follow Eqs. (3.2), (3.3), and (3.4) with $\Gamma = 25$, i.e., as a microcanonical ensemble with Hamiltonian \mathcal{H}_2 . The stress is set equal to zero in one time step at $5500 \Delta t$, the elastic energy is zero after this time. The final $1500 \Delta t$ in Figs. 1–4 are, therefore, for $\Gamma = 0$.

As a consequence of the above described uniaxial loading the system showed characteristic and clearly defined changes in time associated with a structural phase transformation.

As is usual in such studies the structural properties can be readily recognized by quenching the system to essentially zero temperature and then studying the pair correlation function $g(r)$ and the interparticle coordination numbers arising from it. At the end of the calculation displayed in Figs. 1–4 the pair correlation shows unambiguously that the new structure is a close-packed structure with stacking faults. The detailed manner of analyzing close-packed structures and a systematic characterization of close-packed structures will be dealt with in a later paper.

The results of this calculation agrees generally with the results of Parrinello and Rahman² who used the Morse potential and the (HtN) ensemble to study nickel single crystals under a [100] uniaxial compressive load and found a transformation of the same character. In our ongoing studies of this transformation we find that the final state is in general a close-packed structure with stacking faults; and the exact final state obtained depends upon the temperature and the manner in which the stress is applied, that is gradual, as here or as a shock. Here we have shown not only that transformations between different metastable equilibrium states of solids can be studied using the (TtN) equations, but also that in the case reported here the results agree generally with those obtained previously by using the (HtN) theory.

B. Geometrical properties of the transformation

The matrix h in Eq. (3.3) may be constructed from the vectors \mathbf{a} , \mathbf{b} , and \mathbf{c} which define the molecular dynamics cell, and therefore the crystal under study; $h = (\mathbf{a}, \mathbf{b}, \mathbf{c})$.

Before the transformation, that is to the left of 0 in Figs. 1–4, the crystal is defined by the vectors (averaged): $\mathbf{a} = (7.80, 0.00, 0.00)$, $\mathbf{b} = (0.00, 7.80, 0.00)$, and $\mathbf{c} = (0.00, 0.00, 7.80)$. The average density of the system is 1.05.

After the transformation, that is to the right of 7000 in Figs. 1–4, the crystal is defined by the vectors (averaged): $\mathbf{a} = (5.51, 0.00, 0.00)$, $\mathbf{b} = (0.00, 9.30, 1.27)$, and $\mathbf{c} = (0.00, 1.30, 9.48)$. The average density is again 1.05.

Thus, in the course of the structural phase transformation the crystal changes from a cubic volume to a volume defined by the above vectors, both structures having the same average density. The transformation therefore takes place in the following manner: as we compress the system

along the [100] direction the system expands in the directions perpendicular to the [100] direction in such a manner that the change in the average density is small. At the critical stress of $\Gamma \approx 25$ the system responds to the compressive load by reorganizing into a new structure. The value $\Gamma = 25$ corresponds to 135 MPa for argon.

C. Elastic energy

Figure 1 shows the time variation of the elastic energy $V_0 \text{Tr}(\epsilon\epsilon)$, which for this calculation has the form $1/2\Gamma a^2$ where a is the length of the crystal along the [100] direction. The stress is made to increase from time steps: 0 to 500, 1000 to 1250, and 3250 to 3500, which shows up as a steady increase in stored energy over these same intervals. As the stress Γ increases the value of $|a|$ decreases as the system contracts in the [100] direction. At the same time the dimensions perpendicular to [100] direction increase as explained earlier. The phase transformation is clearly shown in this figure as a dramatic drop in the stored energy between time steps 3500 and 3900. Note that the elastic energy is lower at the higher stress $\Gamma = 25$ after the transformation (time steps 4000–5550), than at lower stress $\Gamma = 15$ before the transformation (time steps 1500 to 3000). For such a dramatic decrease in the elastic energy to occur the system must undergo a structural phase transformation. This shows up in the calculation as a change of the shape of the crystal as it reorganizes itself into a more favorable crystalline structure.

D. Temperature

Figure 2 shows the time history of the temperature during the calculation. The temperature fluctuations are 180° out of phase with mass scaling variable f . The change in character of the temperature fluctuations around time step 3500 is obvious from the figure. Here the temperature is responding to the phase transformation. Comparing with Fig. 1 we see that the length a and hence also the volume of the system does not show these long period high amplitude oscillations.

E. Nosé variable f

Figure 3 shows the time history of the Nosé variable f . This variable also clearly signals the onset of the transformation by its rapid rise and larger amplitude oscillations after time step 3500. The variable f responds to the phase transformation in its effort to hold the temperature near $T_0 = 0.15$. The average temperature over the 7000 time step run is 0.148. From time step 0 to time step 3500 the average value of f is 1.07. From time step 4500 to time step 7000 the average of f is 4.59.

F. Mean square displacement

The mean square displacement shown in Fig. 4 is defined by

$$R^2(t) = \sum_a [\mathbf{r}_a(t) - \mathbf{r}_a(t_0)]^2 / (6N),$$

where $\mathbf{r}_a(t)$ is the position of atom a at time t , whereas $\mathbf{r}_a(t_0)$ is the position of atom a at time t_0 . In Fig. 4 $\mathbf{r}_a(t_0)$ is chosen to be the initial fcc lattice positions of the untransformed crystal.

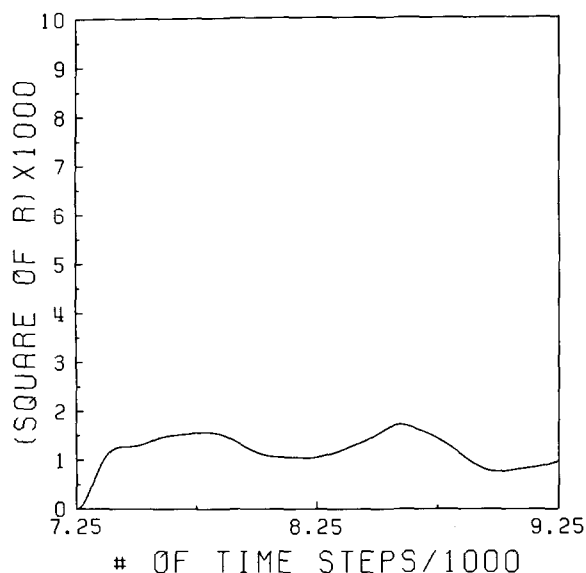


FIG. 5. The mean square displacement for time step 7250 to 9250 using as initial positions those at 7250. This shows the mean square displacement measured with respect to the transformed structure.

Thus R^2 has a small value before the transformation. The change in $R^2(t)$ after the transformation is characteristic of a structural phase transformation; R^2 increases as the atoms reorganize themselves into the new crystal structure.

In order to study R^2 further in the transformed structure we extended the run past time step 7000 with a new choice of $\mathbf{r}_a(t_0)$. By choosing $\mathbf{r}_a(t_0)$ to be the positions of the particles at time step 7250 and evolving the system from time step 7250 to 9250 we obtained the behavior of R^2 shown in Fig. 5. The value of R^2 is lower as expected but it still shows large amplitude and long period oscillations. This is to be compared with R^2 in the untransformed crystal between time steps 0 and 3000 in Fig. 4. The conclusion we reach is that the transformation has excited elastic waves in the crystal which are exhibited by the large amplitude, long period variation of the mean square displacement.

VI. CONCLUSIONS

Following the ideas presented in Andersen's paper⁶ one now has available six different methods of generating-

molecular dynamics ensembles that correspond to the equilibrium ensembles (EhN), (ThN), (HtN), (TtN), (HPN), and (TPN). As has been discussed in Ref. 1 the equations for h have an element of arbitrariness which is apparently not important in the case of equilibrium studies but *may* be important in the case of time correlation studies. Similarly the equations for Nosé's variable f have an element of arbitrariness. For example instead of the kinetic energy for f as in Nosé we could write $\frac{1}{2}g(\Pi)\mathbf{P}^2/M$ where g is some function of Π . These changes in the dynamical equations will change the trajectories in phase space. For equilibrium averages we still obtain the canonical results (3.9) and (4.2), however, time correlation functions could be sensitive to the changes in trajectories.

We have shown that the (TtN) equations may also be used to follow structural phase transformations in systems subjected to external loading. We followed an fcc→close-packed structure phase transformation in a low temperature Lennard-Jones solid using the (TtN) equations. The results were generally the same as obtained earlier using the (HtN) ensemble.

We also mention that Nosé⁴ interprets the factor f to imply a scaling of the time during the simulation. We do not see a compelling reason for this interpretation and have, therefore, proposed the alternative interpretation that f scales the mass of the particle. This puts the new variables h and f on equal footing; h scales particle positions and momenta through the canonical transformation, whereas f scales the particle mass. Also the derivative of the particle Hamiltonian with respect to h is related to the microscopic stress tensor $\mathcal{P}[(\partial\mathcal{H}/\partial h) = -\mathcal{P}A]$; whereas the derivative of the particle Hamiltonian with respect to f is related to the kinetic energy $K[(\partial\mathcal{H}/\partial f) = -2K/f]$. Perhaps future simulations will show which interpretation of the variable f is more useful.

¹J. R. Ray and A. Rahman, J. Chem. Phys. **80**, 4423 (1984).

²M. Parrinello and A. Rahman, J. Appl. Phys. **52**, 7182 (1981).

³R. N. Thurston, in *Physical Acoustics*, edited by W. P. Mason (Academic, New York, 1964), Vol. 2, Part A.

⁴S. Nosé, Mol. Phys. **52**, 255 (1984); J. Chem. Phys. **81**, 511 (1984).

⁵M. Parrinello and A. Rahman, J. Chem. Phys. **76**, 2662 (1982).

⁶H. C. Andersen, J. Chem. Phys. **72**, 2384 (1980).